IJST (2014) 38A3 (Special issue-Mathematics): 355-364
Iranian Journal of Science & Technology

http://ijsts.shirazu.ac.ir

Classification of bounded travelling wave solutions of the generalized Zakharov equation

H. R. Z. Zangeneh[1]*, R. Kazemi[2] and M. Mosaddeghi[1]

[1]*Department of Mathematical Sciences, Isfahan University of Technology, Isfahan, Iran, 84156-83111*
[2]*Department of Mathematical Sciences, University of Kashan, Ravand Road, Kashan, Iran, 87317-53153*
E-mail: hamidz@cc.iut.ac.ir

Abstract

By using bifurcation theory of planar ordinary differential equations all different bounded travelling wave solutions of the Generalized Zakharov equation are classified in different parametric regions. In each of these parametric regions the exact explicit parametric representation of all solitary, kink (anti kink) and periodic wave solutions as well as their numerical simulation and their corresponding phase portraits are obtained.

Keywords*:* Generalized Zakharov equation; travelling wave solutions; Bifurcation theory

1. Introduction

Many phenomena in physics, engineering and science are described by nonlinear partial differential equations (NPDEs). Exact travelling wave solution of nonlinear evolution equation is one of the fundamental objects of study in mathematical physics. When these exact solutions exist, they can help one to understand the mechanism of the complicated physical phenomena and dynamical processes modeled by these nonlinear evolution equations. In the past decades a vast variety of the powerful and direct methods to find the explicit solutions of NPDE have been developed, such as Hirota bilinear method (Hirota, 1971; Hirota, 2004), inverse scattering transform method (M. J. Ablowits 1991), Backlund and Darboux transforms method (Schief 2002), Lie group method (Olver 1993) F-expansion method (Fan 2004), Sine-Cosine method (Yan 1996), homotopy perturbation method (He 2005), homogenous balance method (Wang 1996), algebraic method (Hu 2005), Jacobi elliptic function expansion method (Sh. K. Liu 2001) and dynamical systems point of view (Zh. Dai, 2011; B. Gambo, 2010). Certainly, the bifurcation theory of planar dynamical systems is an efficient method too. In this paper we consider the generalized Zakharov equation by using the bifurcation theory. The Zakharov equations (Zakharov, 1971), are used extensively in considerations of the evolution of Langmuir turbulence when strong turbulence effects are considered. The Zakharov equation has various applications in physics in the theory of deep-water waves (Shemer 2002), communication (Goldman 1984), and nonlinear pulse propagation in fibers (Anderson 1983). The original derivation of these equations was based on a simplified model involving fluid concepts. The model leads to two equations: one of these describes the evolution of the envelop of the Langmuir waves with the nonlinearity included through a term involving a density fluctuation, and the other describes the evolution of the density fluctuation due to the ponder motive force exerted by the Langmuir waves. Now we consider the generalized Zakharov equations which have the form

$$u_{tt} - c_s^2 u_{xx} = \beta(|E|^2)_{xx},\ iE_t + \alpha\, E_{xx} - a_1 uE + a_2|E|^2E + a_3|E|^4E = 0. \quad (1)$$

In (1) α represents the coefficient of dispersion and a_1, a_2, a_3 represent the coefficients of nonlinearity. When $a_2 = a_3 = 0$, (1) reduce to the famous Zakharov equations (see (Zakharov, 1972; Zakharov, 1976) for details) which describe the propagation of Langmuir waves in plasmas. The complex number E represents, the envelop of the electric field, and u is equilibrium value from the fluctuation of the ion density. The parameter c_s is proportional to the ion acoustic speed. We find exact solutions of (1) via the bifurcation theory of planar dynamical systems. The purpose of this paper is to give the bifurcation sets of the bounded travelling wave solutions, i.e., solitary wave

*Corresponding author
Received: 17 August 2013 / Accepted: 12 November 2013

solutions, kink (anti kink) wave solutions and periodic wave solutions. Also, we obtain the explicit representation for some of these solutions in different parametric region determined by the bifurcation set. To find the travelling wave solutions of (1) we consider the travelling wave solutions of the form:

$$E(x,t) = v(\xi)exp[i(kx - \omega t)], u(x,t) = u(\xi), \xi = x - ct, \quad (2)$$

where k, ω, c are arbitrary constants, and c denotes the wave speed, k is the frequency, ω is the soliton wave number and $v(\xi)$ is a real function that represents the shape of the pulse. By substituting for E and u from (2) into the equations (1) we obtain the following ordinary differential equations:

$$(c^2 - c_s^2)u_{\xi\xi} = \beta(v^2)_{\xi\xi}, \alpha v_{\xi\xi} + i(2\alpha k - c)v_\xi + (\omega - \alpha\, k^2)v - a_1\, uv + a_2 v^3 + a_3 v^5 = 0. \quad (3)$$

By integrating the first equation in (3) twice with respect to ξ and taking the integration constant to be zero we obtain

$$u = \frac{\beta}{(c^2 - c_s^2)} v^2; \quad (4)$$

Now we substitute (4) in the second equation of (3) to obtain

$$v_{\xi\xi} + av + bv^3 + \gamma\, v^5 = 0 \quad (5)$$

where

$$a = \frac{(\omega - \alpha\, k^2)}{\alpha}, \quad b = \frac{a_2}{\alpha} - \frac{\beta\, a_1}{(c^2 - c_s^2)}, \quad \gamma = \frac{a_3}{\alpha}, \quad c = 2\alpha\, k \quad (6)$$

Now let $dv/d\xi = y$. Then we derive the following travelling wave system which is a planar Hamiltonian system

$$\dot{v} = y$$
$$\dot{y} = -v(a + bv^2 + \gamma v^4). \quad (4)$$

Because the phase portraits of the Hamiltonian system (7) determine travelling wave solutions of (1), we find the bifurcation set for which the qualitative behavior of phase portraits of (7) changes. Here we consider only bounded travelling waves because in physical model only bounded travelling waves are meaningful. Suppose that $v(x,t) = v(x - ct) = v(\xi)$ is a continuous solution of system (7) for $-\infty < \xi < \infty$ and $\lim_{\xi \to +\infty} v(xi) = p$, $\lim_{\xi \to -\infty} v(\xi) = q$. We recall that

(i) if $p = q$ then $v(x,t)$ is called a solitary or impulse wave solution, and

(ii) if $p \neq q$ then $v(x,t)$ is called kink(anti kink) wave solution.

Usually a solitary wave solution, a kink (anti kink) wave and periodic travelling wave solutions of equations (1) correspond to a homoclinic orbits or cuspidal loop, heteroclinic orbit or eye figure loop and periodic orbit of (7) respectively. Thus it is necessary to find all periodic orbits, homoclinic orbits, heteroclinic orbits of system (7) which depend on the systems' parameters.

The rest of this paper is organized as follows. In section 2, we give the bifurcation set and corresponding phase portrait of system (7). In Section 3, using the information obtained about the phase portraits of bounded solutions of (7) we obtain the numerical simulation for corresponding bounded travelling wave solutions of the system (1). In Section 4, exact explicit parametric representation for different possible solitary wave solutions, periodic travelling wave solutions and kink (anti kink) wave solutions of equation (1) are given.

2. Bifurcation in phase portrait of (7)

In this section, first a brief definition of the bifurcation is given. Bifurcation means changes in qualitative structure of the flow of a differential equation as parameter changes (J. K. Hale and H. Kocak 1991). Thus a bifurcation is a change of the topological type of the system as the parameters pass through a bifurcation value (kuznetsov 1998). We will often refer as local bifurcations to bifurcations that happen in any small neighborhood of the equilibria or cycles. There are also bifurcations that cannot be detected by looking at small neighborhood of equilibria or cycles. Such bifurcations are called global. In our analysis we consider both local and global bifurcations.

Now we consider bifurcation set (set of bifurcation values of parameters) and qualitatively different phase portraits of (7). First the generic case $\gamma \neq 0$ is considered With some time scaling and without loss of generality we can assume $\gamma = \pm 1$, so that we can have Hamiltonian system

$$\dot{v} = y,$$
$$\dot{y} = -v(a + bv^2 \pm v^4) := f_{\pm(v)}. \quad (8)$$

with Hamiltonian $H_\pm(v,y) = y^2/2 + F_\pm(v)$, where $\pm$ correspond to $\gamma = \pm 1$ and $F_\pm(v) = \pm v^6/6 + b\, v^4/4 + av^2/2$ is the corresponding potential function. It is clear that critical points of $F_\pm$ are zeros of $f_\pm$, since $-f_\pm$ are derivatives of $F_\pm$. It is known that isolated minimum, maximum and inflection points of F correspond to center, saddle point and cusp point of system (8), respectively (e.g. see (J. K. Hale and H. Kocak 1991). Also, it is known that the global structure of phase portraits of system (8) will not change qualitatively unless one of

the conditions listed below is violated (J. K. Hale and H. Kocak 1991):

i. There are only finitely many critical points of $F_{\pm}$.

ii. Each critical point of $F_{\pm}$ is non-degenerate, that is $F''_{\pm}(\bar{v}_1) \neq 0$ for critical point $\bar{v}_1$.

iii. No two maximum values of $F_{\pm}$ are equal.

iv. $|F_{\pm}(v_1)| \to \infty$ as $|v_1| \to \infty$, that is $F_{\pm}$ is unbounded for both $v_1 \to \infty$ and $v_1 \to -\infty$.

Potential functions satisfying the above four conditions are called the generic potential functions. In our case it is clear that conditions i and iv are satisfied for all values of a and b. Therefore to find the bifurcation set, we first need to find conditions where critical points of $F_{\pm}$ become degenerate. So we set

$$f_{\pm}(a,b,v) = av + b\,v^3 \pm v^5 = 0, \quad (9)$$

$$\frac{\partial f_{\pm}(a,b,v)}{\partial v} = a + 3bv^2 \pm 5v^4 = 0.) \quad (10)$$

By solving (9) and (10) we find the bifurcation set to be $B_+ = \{(a,b): a = 0, b^2 = 4a, b < 0\}$ and $B_- = \{(a,b): a = 0, b^2 = -4a, b > 0\}$ which correspond to $\gamma = \pm 1$ respectively. These bifurcation sets divides the parametric plane into 7 distinct regions (see Figs. 1 and 2). In each parametric regions, the number and type of the critical points remain unchanged. To see the type and number of critical points it is sufficient to consider only a typical equation for a particular value of a and b in each region. Critical points of $F_{\pm}$ are $v = 0$ and $v = \pm\sqrt{(-b \pm \sqrt{\Delta_{\pm}})/(\pm 2)}$ where $\Delta_{\pm} = b^2 \mp 4a$ which correspond to $\gamma = \pm 1$ respectively. It is easy to verify that number of critical points of $F_{\pm}$ will change from one non-degenerate critical point in region III to five non-degenerate critical points in region (I) and three non-degenerate critical points in region (V). On the boundary of these regions, i.e. regions II, IV, VI and VII critical points are degenerate. To classify the critical points and determine the phase portraits of system (7) we need to consider two cases $\gamma = 1$ and $\gamma = -1$ separately.

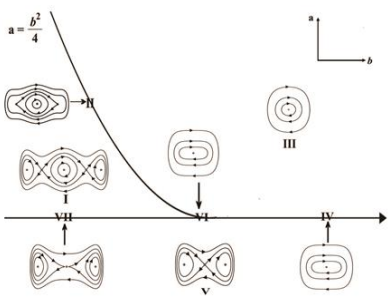

Fig. 1. Bifurcation sets and phase portraits of equation (8) with $\gamma = 1$ in different parametric regions

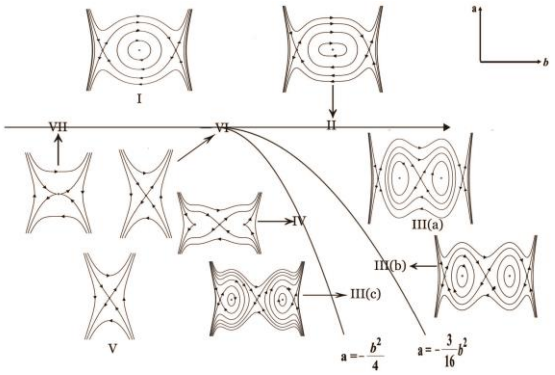

Fig. 2. Bifurcation sets and phase portraits of equation (8) with $\gamma = -1$ in different parametric regions

Case I. $\gamma = 1$

Since F is a sixth order polynomial and the coefficient of v^6 is positive, it is easy to verify that the only non-degenerate critical points of F in region III($\Delta_+ < 0$; or $\Delta_+ \geq 0, b > 0, a > 0$) is $v = 0$ which is a minimum point. Therefore, in this region system (7) has a global center (see Fig. 1).

In region II ($\Delta^+ = 0, \mathrm{b} < 0$), F_+ has three critical points where $v = 0$ is a minimum and $v = \pm\sqrt{-b/2}$ are inflection points. These points correspond to a center and cusp points of (7) respectively. Also, because of symmetry, $H_+(\sqrt{-\frac{b}{2}}, 0) = H_+(-\sqrt{-\frac{b}{2}}, 0) > H(0,0)$. Therefore system (7) will have an eye-figure loop connecting the cusp points and an oval of periodic orbits encircling the origin and also a band of periodic orbits outside the eye-figure loop (see Fig. 1).

In region I ($\Delta_+ > 0, \mathrm{b} < 0, \mathrm{a} > 0$) the potential function F_+ always has three non-degenerate minimum points and two non-degenerate maximum points between them. Therefore, in this region system (7) has three center and two saddle points.

Since F_+ is even and the critical points $\pm\sqrt{(-b - \sqrt{\Delta_+})/2}$ are symmetric with respect to a-axis we have

$$F_+\left(\sqrt{\frac{-b-\sqrt{\Delta_+}}{2}}\right) = H_+\left(-\sqrt{\frac{-b-\sqrt{\Delta_+}}{2}}, 0\right).$$

There will be an orbit, heteroclinic to these two saddle points, and since

$$H_+(0,0) < H_+\left(\pm\sqrt{(-b - \sqrt{\Delta_+})/2}, 0\right),$$

this heteroclinic cycle includes a band of periodic orbits encircling the origin.

Also,

since $H_+\left(-\sqrt{\frac{-b-\sqrt{\Delta_+}}{2}},0\right) > H_+(-\sqrt{\frac{-b+\sqrt{\Delta_+}}{2}},0)$ and $H_+(\sqrt{\frac{-b-\sqrt{\Delta_+}}{2}},0) > H_+(\sqrt{\frac{-b+\sqrt{\Delta_+}}{2}},0)$, there will be two orbits homoclinic to these saddle points. These homoclinic orbits include a band of periodic orbits encircling centers at $(\pm\sqrt{\frac{-b+\sqrt{\Delta_+}}{2}},0)$ points in system (7) (see Fig. 1).

In regions IV ($b > 0, a = 0$), and VI, $a = b = 0$ the only critical point of F_+ is $v = 0$ which is a degenerate minimum point, therefore system (7) has a global degenerate center at origin (see Fig. 1).

In region V ($a < 0$), F_+ has three non-degenerate critical points at $v = 0, v = \pm\sqrt{(-b+\sqrt{\Delta_+})/2}$, where $v = 0$ is a maximum and $v = \pm\sqrt{(-b+\sqrt{\Delta_+})/2}$ are minimum points. Also $H_+(0,0) > H\left(\pm\sqrt{\frac{-b+\sqrt{\Delta_+}}{2}},0\right)$. Therefore, system (7) has orbits double homoclinic to saddle point at the origin. Also, there will be ovals of periodic orbits inside each of the homoclinic orbits encircling centers at $(\pm\sqrt{(-b+\sqrt{\Delta_+})/2},0)$ and a band of periodic orbits outside the double homoclinic (figure eight-loop) orbits (see Fig. 1).

In region VII ($a = 0, b < 0$), situation is similar to that of region V with the difference that, the maximum point of F_+ and saddle point of system (7) is degenerate in this case. (see Fig. 1).

Therefore, we have proved the following lemma:

Lemma1. Phase portrait of system (7) corresponding to $H_+ = h$ is classified as follows (see Fig. 1):

i. In region I ($\Delta_+ > 0, a > 0, b < 0$), phase portrait of system (8) consists of two saddle points, three centers, a cycle heteroclinic to saddle points, two orbits homoclinic to saddle points and bands of periodic orbits inside the heteroclinic cycle and homoclinic orbits, and outside of figure eight-loop.

ii. In region (II) ($\Delta_+ = 0, b < 0$) phase portrait of (7) consists of a center, two cusp points, an eye-figure loop and two bands of periodic orbits inside and outside of the eye-figure loop.

iii. In regions III ($\Delta_+ < 0$ or $\Delta_+ \geq 0,\ a > 0,\ b > 0$) phase portrait consists of a global non-degenerate center.

iv. In regions VI ($a = b = 0$) and IV ($a = 0, b > 0$), phase portrait consists of a degenerate global center.

v. In region $V(a < 0)$, phase portrait consists of a non-degenerate saddle point at the origin, two centers at $(\pm\sqrt{(-b+\sqrt{\Delta_+})/2},0)$, a double homoclinic orbit to the saddle point and bands of periodic orbits inside and outside of the double homoclinic orbit.

vi. In region VII ($a = 0, b < 0$), phase portrait consist of a degenerate saddle point at the origin, two centers, a double homoclinic orbit to the saddle point and bands of periodic orbits inside and outside of the double homoclinic orbit.

Case II. $\gamma = -1$

In this case parametric region is divided into eight locally topologically equivalent regions by bifurcation set B_- (see Fig. 2). Using a similar analysis to Case I we can derive the phase portraits of system (7). In region III ($\Delta_- > 0,\ a < 0, b > 0$) potential function F_- has three non-degenerate maximum points at $x = 0,\ x = \pm\sqrt{\frac{b+\sqrt{\Delta_-}}{2}}$ and two minimum points at $x = \pm\sqrt{\frac{b-\sqrt{\Delta_-}}{2}}$. Also, because of symmetry $H_-\left(\sqrt{\frac{b+\sqrt{\Delta_-}}{2}},0\right) = H_-\left(-\sqrt{\frac{b+\sqrt{\Delta_-}}{2}},0\right)$. Therefore saddle points $\pm\left(\sqrt{(b+\sqrt{\Delta_-})/2},0\right)$ always lies on the same level curve of the Hamiltonian $H_- = h$. Furthermore along parabola $a = -3b^2/16, b > 0$ all three saddle points lie on the same potential level, i.e. $H(0,0) = H\left(\sqrt{(b+\sqrt{\Delta_-})/2},0\right) = 0$, therefore region III will be divided into three subregions which will be denoted by

III $(a) = \left\{(a,b) \in \text{region III: } a > -\frac{3b^2}{16}\right\}$,

III (b) = $\left\{(a,b) \in \text{region III: } a = -\frac{3b^2}{16}\right\}$ and

III(c) = $\left\{(a,b) \in \text{region III: } a < -\frac{3b^2}{16}\right\}$. In region III(b) bounded orbits of phase portraits of system (7) consist of two cycles heteroclinic to saddle points at origin and $\left(\sqrt{(b+\sqrt{\Delta_-})/2},0\right)$, and bands of periodic orbit inside the heteroclinic cycles. In region III(a), $0 = H(0,0) < H_-\left(\pm\sqrt{(b+\sqrt{\Delta_-})/2},0\right)$, therefore the phase portrait of bounded orbits of (7) consist of a double homoclinic orbit to origin, a cycle heteroclinic to saddle points $\left(\pm\sqrt{(b+\sqrt{\Delta_-})/2},0\right)$, bands of periodic orbits inside homoclinic orbits and a band of periodic orbits outside oh double homoclinic orbit and inside the heteroclinic cycles. In region

III(c), $0 = H(0,0) > H_-\left(\pm\sqrt{\frac{b+\sqrt{\Delta_-}}{2}}, 0\right)$. Therefore the phase portraits of bounded periodic orbits consist of homoclinic orbits to saddle points $\left(\pm\sqrt{\frac{b+\sqrt{\Delta_-}}{2}}, 0\right)$ and band of periodic orbits inside each of the homoclinic orbits (see Fig. 2). Phase portraits of system (7) in other regions are derived in a similar manner and are omitted here for the sake of brevity. Therefore, it is proved that:

Lemma2. Phase portrait of system (7) corresponding to $H_- = h$ is classified as follows (see Fig. 2):
i. In region I $(a > 0)$ phase portrait of bounded orbits consists of a center at the origin, two saddle points at $\left(\pm\sqrt{(b+\sqrt{\Delta_-})/2}, 0\right)$, cycle heteroclinic to the saddle points and a band of periodic orbits encircling the origin inside the heteroclinic cycle.
ii. In region II $(a = 0, b > 0)$, phase portrait of bounded orbits consists of a degenerate center at the origin, two saddle points at $(\pm\sqrt{b}, 0)$, cycle heteroclinic to the saddle points and a band of periodic orbits encircling the origin inside the heteroclinic cycle.
iii. In region (III) $(\Delta_- > 0, a < 0, b > 0)$, there are three saddle points at (0,0), $\left(\pm\sqrt{(b+\sqrt{\Delta_-})/2}, 0\right)$ and two centers at $\left(\pm\sqrt{(b-\sqrt{\Delta_-})/2}, 0\right)$. In regions III(a) there are a double homoclinic orbit to origin, a cycle heteroclinic to saddle points $\left(\sqrt{\frac{b+\sqrt{\Delta_-}}{2}}, 0\right)$, bands of periodic orbits inside homoclinic orbits and a band of periodic orbits outside double homoclinic orbit and inside the heteroclinic cycles. In region III (b) there are two cycles heteroclinic to saddle points at origin and $\left(\sqrt{\frac{b+\sqrt{\Delta_-}}{2}}, 0\right)$, and bands of periodic orbit inside the heteroclinic cycles. In region III(c), there are homoclinic orbits to saddle points $\left(\pm\sqrt{(b+\sqrt{\Delta_-})/2}, 0\right)$ and band of periodic orbits inside each of the homoclinic orbits.
iv. In region IV $(\Delta_- = 0,\ b > 0,\ a < 0)$, there is a saddle point at $(0,0)$ and two cusp points at $(\pm\sqrt{b/2}, 0)$.
v. In region V $(\Delta_- < 0\ or\ \Delta_- \geq 0,\ \mathrm{a} < 0, \mathrm{b} < 0)$ there is only a saddle point at $(0,0)$.
vi. In regions VII $(a = 0, b < 0)$ and VI $(a = b = 0)$, there is a non hyperbolic saddle point at the origin $(0,0)$.

Case III. $\gamma = 0$
Now we consider the degenerate case $\gamma = 0$. If $b \neq 0$, equation (7) becomes

$$\dot{v} = y,$$
$$\dot{y} = -v(a + bv^2). \quad (11)$$

Then without loss of generality we can assume $b = \pm 1$, so that we can have Hamiltonian system

$$\dot{v} = y,$$
$$\dot{y} = -v(a \pm v^2) := \tilde{f}_{\pm}(v), \quad (12)$$

with Hamiltonian $\tilde{H}_{\pm}(v, y) = y^2/2 + \tilde{F}_{\pm}(v)$, where $\pm$ corresponds to $b = \pm 1$ and $\tilde{F}_{\pm}(v) = \pm v^4/4 + av^2/2$ is the corresponding potential function. Similar to the above discussions to the case I and II, we see that bifurcation occurs in $a = 0$. If $\gamma = b = 0$ then system (5) becomes a linear differential equation. Then we have the following lemma:

Lemma3. Phase portrait of system (11) corresponding to $\tilde{H}_{\pm} = h$ is classified as follows:
i. If $b = 1$ then the phase portrait of system (11) consists of a global center at the origin for $a > 0$, a degenerate global center at the origin for $a = 0$ and a non-degenerate saddle point at the origin, two centers at $(\pm\sqrt{-a}, 0)$, a double homoclinic orbit to the saddle point and bands of periodic orbits inside and outside of the double homoclinic orbit for $a < 0$.
ii. If $b = -1$ then the phase portrait of system (11) consists of two non-degenerate saddle points at $(\pm\sqrt{a}, 0)$, cycle heteroclinic to the saddle points and a band of periodic orbits encircling the origin inside the heteroclinic cycle for $a > 0$, a degenerate saddle at the origin for $a = 0$ and a saddle at the origin for $a < 0$.
iii. If $b = 0$ then for $a = 1$ we have a global center at the origin and for $a = -1$ we have a non-degenerate saddle point at the origin.

3. The numerical simulation of bounded travelling waves

It is well known that the bounded travelling waves $E(\xi)$ of system (1) correspond to the bounded integral curves of system (7). In Lemmas 1, 2 and 3, all bounded integral curves of system (7). have been classified. In this section we give numerical simulation for a typical member of bounded travelling waves of system (7) in the form of $v(x,t) = v(x - ct) = v(\xi)$ as follows:
Case I. Homoclinic loops
These orbits only exist in regions I, V when $\gamma =$

1, in regions III(a), III(c) when $\gamma = -1$ and for $\gamma = 0, a < 0$. Homoclinic orbits of system (7) correspond to solitary travelling waves of (5). Let $\gamma = 1,\ b = -3,\ a = 7/4,$ which correspond to a point in region I of Fig. 1. Now we consider system (7) and choose initial conditions $v(0) = -1.707106,\ v'(0) = 0$. So that they lie on the left branch of double homoclinic orbit (figure-eight loop). In physics this type of travelling wave is called solitary wave with valley form (see Fig. 3(a)). Now let $\gamma = 1,\ b = -3,\ a = 7/4$ which correspond to a point in parametric region I in Fig. 1. Again we use initial conditions to be on the homoclinic orbit of system (7). Let $v(0) = 1.707106, v'(0) = 0$ so that they lie on the right branch of double homoclinic orbit (figure-eight loop). This type of travelling wave in physics is called solitary wave with peak form (see Fig. 3(b)).

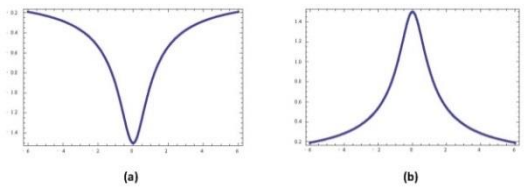

Fig. 3. The simulation of solitary waves corresponding to the homoclinic orbits of equation (7). (a) Solitary wave of valley form, (b) Solitary wave of peak type

Case II. Nilpotent Homoclinic loops

These orbits only exist in region VII when $\gamma = 1$. Nilpotent Homoclinic loop of system (7) corresponds to solitary wave of system (5). As in the previous part two set of parameters $\gamma = 1,\ b = -\frac{3}{2},\ a = 0$ are chosen which correspond to a point in region VII in Fig. 1. Now we consider system (7) and choose initial conditions $v(0) = -1.066517046,\ v'(0) = 0$ so that they lie on the left branch of degenerate double homoclinic (figure eight loop) which correspond to solitary wave with valley form (see Fig. 4(a)). For the same parameters and initial conditions $v(0) = 1.066517046,\ v'(0) = 0$ so that they lie on the right branch of degenerate double homoclinic (figure eight loop) which correspond to solitary wave with peak form (see Fig. 4(b)).

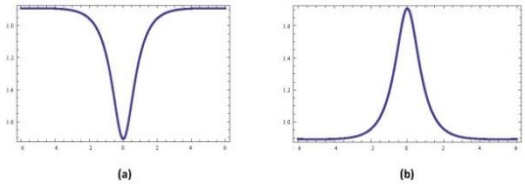

Fig. 4. The simulation of the solitary waves corresponding to nilpotent homoclinic orbits of equation (7). (a) Solitary wave of valley form, (b) Solitary wave of peak form

Case III. Heteroclinic orbits

These orbits exist only in region I when $\gamma = 1$ and in regions I, II, III(b) when $\gamma = -1$ and for $\gamma = 0, a > 0$. Upper and lower heteroclinic orbits of system (7) correspond to kink and anti-kink travelling waves of system (5) respectively. Again we consider system (7) and choose $\gamma = 1, b = -3, a = 7/4$ which correspond to a point in parametric region I in Fig. 1. As has been mentioned above in this case we have orbits are heteroclinic to saddle points $\left(-\sqrt{(3-\sqrt{2})/2}, 0\right)$ and $\left(\sqrt{(3-\sqrt{2})/2}, 0\right)$. Now we use initial conditions $v(0) = 0, v'(0) = 0.7814744144$ and $v(0) = 0, v'(0) = -0.7814744144$ on upper and lower heteroclinic orbits respectively and obtain Fig. 5(a, b).

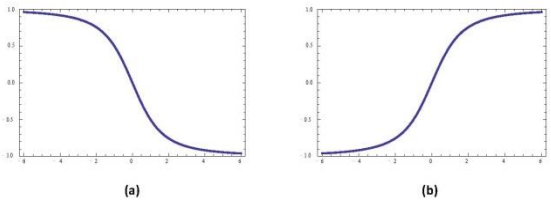

Fig. 5. The simulation of the kink and anti-kink waves corresponding to the heteroclinic orbits of equation (7). (a) Anti-kink waves, (b) Kink waves

Case IV. Eye-figure loop

This loop exists only in region II when $\gamma = 1$. Upper and lower orbits of eye-figure loop of system (7) again correspond to kink and anti-kink travelling waves of system (5) respectively. As in previous part a set of parameters $\gamma = 1,\ b = -2,\ a = 1$ are chosen, which correspond to a point in region II in Fig. 1. Now we consider system (7) and choose initial conditions $v(0) = 0, v'(0) = 0.5773502692$ and $v(0) = 0, v'(0) = -0.5773502692$ on upper and lower orbits of eye-figure loop respectively and obtain Fig. 6 (a, b).

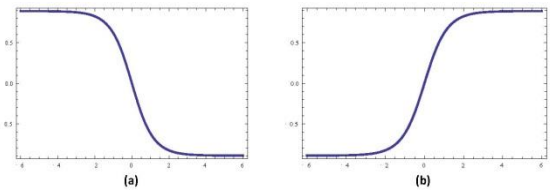

Fig. 6. The simulation of the kink and anti-kink waves corresponding to the eye figure loop of equation (7). (a) Anti-kink waves, (b) Kink waves

Case V. Periodic orbit

These periodic orbits are global (regions III, IV, VI) when $\gamma = 1$ and for $\gamma = 0, b = 1, a \geq 0$ or

local which lie inside homoclinic orbits (regions I,V) when $\gamma = 1$ and (regions III(a), III(c)) when $\gamma = -1$, inside and outside of eye-figure loop (regions II) when $\gamma = 1$, inside heteroclinic cycles (region I) when $\gamma = 1$ and (region I, II, III(b)) when $\gamma = -1$ and for $\gamma = 0,\ b = -1,\ a > 0$, inside and outside of double figure-eight loop (regions I) when $\gamma = 1$, inside and outside of nilpotent double homoclinic loop, (regions VII) when $\gamma = 1$ and inside and outside of figure eight loop (regions III(a)) when $\gamma = -1$ and for $\gamma = 0,\ b = 1,\ a < 0$. Periodic orbits of system (7) correspond to periodic travelling waves of system (5). Here we choose a periodic orbit inside the heteroclinic orbits in region I in Fig. 1. Of course, we could choose a global center or period orbits inside homoclinic orbits, period orbits inside and outside of eye figure loop as well, but the figures are qualitatively the same. Let $\gamma = 1, b = -3, a = 7/4$. Heteroclinic orbit corresponding to these set of parameters passes through saddle points $\left(-\sqrt{(3-\sqrt{2})/2}, 0\right)$ and $\left(\sqrt{(3-\sqrt{2})/2}, 0\right)$ and include the center $(0,0)$ of system (7). We choose three sets of initial conditions $v(0) = 0,\ v'(0) = 0.7, v(0) = 0,\ v'(0) = 0.000001$ and $v(0) = 0,\ v'(0) = 0.7811,$ close to center $(0,0)$, somewhere in the middle and very close to heteroclinic orbit respectively (see Fig. 7 (a, b, c)). We notice that the period of these periodic orbits increases as we move away from the center toward the heteroclinic orbits. When $\gamma = 1$ we choose two set of initial conditions $v(0) = 1.523, v'(0) = 0$ and $v(0) = 1.7,\ v'(0) = 0$ close and far from the figure-eight loop in region V respectively (see Fig. 8(a, b)). Finally, we choose two sets of initial conditions $v(0) = 0, v'(0) = 0.82$ and $v(0) = 0, v'(0) = 1.5$ close and far from the double figure-eight loop respectively (see Fig. 9(a, b)).

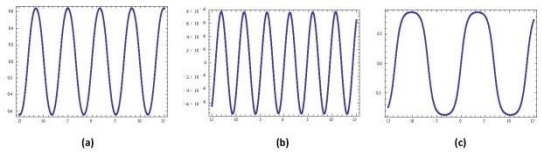

Fig. 7. Simulation of periodic waves corresponding to periodic orbits inside heteroclinic cycle of equation (7). (a) Medium period, (b) Short period, (c) Long period

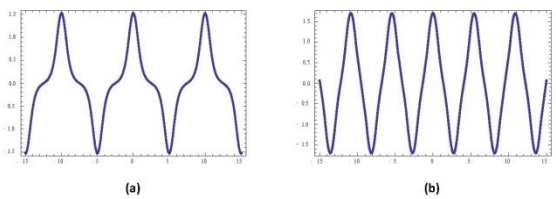

Fig. 8. Simulation of periodic waves corresponding to periodic orbits outside of figure-eight loop of equation (7). (a) Close to figure-eight loop, (b) Far from figure-eight loop

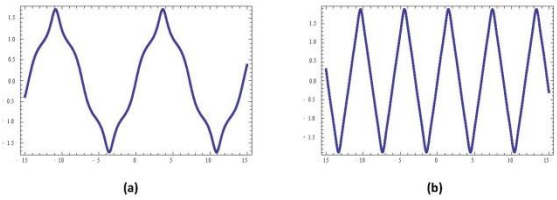

Fig. 9. Simulation of periodic waves corresponding to periodic orbits outside of double eight figure loop of equation (7). (a) close to double figure-eight loop, (b) Far from double figure-eight loop

Remark 1.

i. We notice the difference between solitary waves in Figs. 3 and 4 and kink, anti-kink in Figs. 5 and 6 which shows their asymptotic behavior as $t \to \pm\infty$. In Fig. 3 stable and unstable manifolds of equilibrium point intersect transversally but in Fig. 4 they intersect tangentially. Similar condition holds in Figs. 5 and 6 respectively.

ii. We notice that the number of inflection points on periodic waves during one half period in each of Figs. 7, 8 and 9 is zero, one and two which correspond to the shape periodic orbits of system (7).

4. Explicit formulas for bounded integral curves of (7)

In this section explicit formulas for bounded travelling waves of system (7) are given. In the first step we consider the bounded graphics of system (7).

CASE 1. $\gamma = +1$

Region **I:** There are two homoclinic orbits and two heteroclinic orbits of system (7) defined by $H(v,y) = H\left(\pm\sqrt{(-b+\sqrt{\Delta_+})/2}, 0\right) = H(\pm\bar{v}, 0)$ connecting saddle points $(\pm\bar{v}, 0)$ which are passing through points $(\pm\,\tilde{v}, 0)$. Therefore $y = \pm\sqrt{2(H(\bar{v},0) - H(v,0))} = \pm|v^2 - \bar{v}^2|\sqrt{(\tilde{v}\hat{}2\ - v^2)/3}$, where $\tilde{v} = \sqrt{(-b+2\sqrt{\Delta_+})/2}$ and $\bar{v} = \sqrt{(-b+\sqrt{\Delta_+})/2}$. On the right and down branch of the homoclinic orbit we have $y = (v^2 - \bar{v}^2)\sqrt{(\tilde{v}\hat{}2\ - v^2)/3}$. Since $dv/d\xi = y$, by integrating along the right homoclinic orbit for negative y we get:

$$\int_0^{\xi} d\zeta = \sqrt{3}\int_v^{\tilde{v}} \frac{d\phi}{(\phi^2 - \bar{v}^2)\sqrt{\tilde{v}^2 - \phi^2}}.$$

Then after some algebraic calculations we obtain solitary wave solutions:

$$v(\xi) = \pm \frac{\bar{v}\tilde{v}}{\sqrt{(\tilde{v}^2 - \bar{v}^2)\tanh^2\left(\bar{v}\xi\sqrt{\frac{\tilde{v}^2 - \bar{v}^2}{3}} + \bar{v}^2\right)}}.$$

Along the above heteroclinic orbit we have $y = (\bar{v}^2 - v\text{^}2)\sqrt{(\tilde{v}^2 - \bar{v}^2)/3}$. As above we can obtain kink and anti-kink wave solutions:

$$v(\xi) = \pm \frac{\bar{v}\tilde{v}\tanh\left(\bar{v}\xi\sqrt{(\tilde{v}^2 - \bar{v}^2)/3}\right)}{\sqrt{\tilde{v}^2 + \bar{v}^2\left(\tanh^2\left(\bar{v}\xi\sqrt{(\tilde{v}^2 - \bar{v}^2)/3}\right) - 1\right)}}$$

Region **II.** There is an eye-figure loop of system (7) defined by $H(v,y) = H(\sqrt{-b/2}, 0) = H(\pm\bar{v}, 0)$, connecting the cuspidal points $(\pm\bar{v}, 0)$. Therefore $y = \pm\sqrt{(\bar{v}^2 - v^2)^3/3}$. Along the above heteroclinic orbit we have $y = (\bar{v}^2 - v^2)\sqrt{(\bar{v}^2 - v^2)^3/3}$, which have kink and anti-kink solutions:

$$v(\xi) = \pm \frac{\xi\bar{v}^3}{\sqrt{3 + \xi\text{^}2\bar{v}^4}}.$$

Region **V.** There are two orbits homoclinic to origin for system (7) defined by $H(v,y) = 0$ that are passing through points $(\pm\bar{v}, 0)$. Therefore $y = \pm|v|\sqrt{(\bar{v}^2 - v^2)(v^2 + k^2)/3}$, where $\bar{v} = \sqrt{-3b/4 + \sqrt{9b^2 - 48a}/4}; k^2 = 3b/4 + \sqrt{9b^2 - 48a}/4$. The solitary wave solutions are:

$$v(\xi) = \pm \frac{\sqrt{2}\bar{v}k}{\sqrt{(k^2 - \bar{v}^2) + (k^2 + \bar{v}^2)\cosh(2\bar{v}k\xi/\sqrt{3})}}.$$

Region **VII.** There are two nilpotent homoclinic orbits of system (7), defined by $H(v,y) = 0$ connecting to degenerate saddle point (0,0) and passing through points $(\pm\bar{v}, 0)$. Then we have $y = \pm\sqrt{v^4(\tilde{v}^2 - v^2)} = \pm v^2\sqrt{(\tilde{v}^2 - v^2)/3}$ where $\tilde{v} = \sqrt{-3b/2}$. The solitary wave solutions are:

$$v(\xi) = \pm \frac{\sqrt{3}\tilde{v}}{\sqrt{3 + \tilde{v}^4\xi^2}}.$$

CASE 2. $\gamma = -1$

Region **I**: There are two heteroclinic orbits of system (7), defined by $H(v,y) = H(\pm\bar{v}, 0) = H\left(\pm\sqrt{(b + \sqrt{\Delta^-})/2}, 0\right)$ connecting the with two saddle points $(\pm\bar{v}, 0)$. Therefore $y = \pm(\bar{v}^2 - v^2)\sqrt{(v^2 + k^2)/3}$, where $k^2 = -b/2 + \sqrt{\Delta^-}$, which have kink and anti-kink solutions:

$$v(\xi) = \pm \frac{\bar{v}k\tanh\left(\bar{v}\xi\sqrt{\bar{v}^2 + k^2/3}\right)}{\sqrt{k^2 + \bar{v}^2\left(1 - \tanh\left(\bar{v}\xi\sqrt{\bar{v}^2 + k^2/3}\right)\right)}}$$

Region **II.** There are two heteroclinic orbits of system (7), defined by $H(v,y) = H(\pm\sqrt{b}, 0)$ connecting with two saddle points $(\pm\sqrt{b}, 0)$. Therefore $y = \pm(b - v^2)\sqrt{(v^2 + b/2)/3}$. The kink and anti-kink solutions are given by:

$$v(\xi) = \pm \frac{\sqrt{b}\tanh(b\xi/\sqrt{2})}{\sqrt{3 - 2\tanh^2(b\xi/\sqrt{2})}}.$$

Region **III(a).** There are two homoclinic orbits of system (7) defined by $H(v,y) = 0$ connecting with saddle point (0,0) and passing through points $(\pm\bar{v}, 0)$. Therefore $y = \pm|v\sqrt{(v^2 - \bar{v}^2)(v^2 - k^2)/3}$ Where $\bar{v} = \sqrt{3\mathrm{b} - \sqrt{9\mathrm{b}^2 + 48\mathrm{a}}}/2$ and $k\sqrt{3\mathrm{b} + \sqrt{9\mathrm{b}^2 + 48\mathrm{a}}}/2$. We have two solitary wave solutions:

$$v(\xi) = \pm \frac{2\bar{v}\,k\sqrt{k\text{^}2 - \bar{v}\text{^}2}\exp(\xi\bar{v}\,k/\sqrt{3})}{\sqrt{\left[(k^2 - \bar{v}^2)\exp(2\xi\bar{v}\,k/\sqrt{3})\right]^3 - 4\bar{v}^2k^2}}.$$

In this region there are also two heteroclinic orbits of system (7) defined by $H(v,y) = H(\pm\tilde{v}, 0) = H\left(\pm\sqrt{(b + \sqrt{\Delta_-})/2}, 0\right)$ connecting the saddle points $(\pm\tilde{v}, 0) = \left(\pm\sqrt{(b + \sqrt{\Delta_-})/2}, 0\right)$. Therefore $y = \pm(\tilde{v}^2 - v^2)\sqrt{(v^2 + m^2)/3}$, where $k^2 = (-b + 2\sqrt{\Delta_-})/2$. Kink and anti-kink solutions are given by:

$$v(\xi) = \pm \frac{m\tilde{v}\tanh(\tilde{v}\sqrt{(\tilde{v}^2 + m^2)/3}\xi)}{\sqrt{m^2 + \tilde{v}^2\left(1 - \tanh^2(\tilde{v}\sqrt{(\tilde{v}^2 + m^2)/3}\xi)\right)}}.$$

Region **III (b).**

There are four heteroclinic orbits of system (8) defined by $H(v,y) = H(0,0)$. Two of these orbits connect (0,0) and $\left(-\sqrt{(b + \sqrt{\Delta_-})/2}, 0\right)$ and the other two connect (0,0) and $\left(\sqrt{(b + \sqrt{\Delta_-})/2}, 0\right)$. Therefore $y = \pm\sqrt{(\bar{v}^2 - v^2)^2v^2/3} = \pm(\bar{v}^2 - v^2)v/\sqrt{3}$, where $\bar{v} = \sqrt{(b + \sqrt{\Delta_-})/2}$. Kink and anti-kink solutions are of the form:

$$v(\xi) = \pm \frac{\bar{v}\,\tilde{v}\exp(\bar{v}^2\xi/\sqrt{3})}{\sqrt{\bar{v}^2 + \tilde{v}^2\left(\exp(2\bar{v}^2\xi/\sqrt{3}) - 1\right)}},$$

where $\tilde{v} = \sqrt{(b - \sqrt{\Delta_-})/2}$.

Region **III (c):**

There are two homoclinic orbits of system (7) defined by $H(v,y) = H(\pm\sqrt{(b+\sqrt{\Delta_-})/2}, 0) = H(\pm\bar{v}, 0)$ connecting with saddle points $(\pm\bar{v}, 0)$ and passing through points $(\pm\tilde{v}, 0)$. Therefore $y = \pm(\bar{v}^2 - v^2)\sqrt{(v^2 - \tilde{v}^2)/3}$ where $\bar{v} = \sqrt{(b+\sqrt{\Delta_-})/2}$ and $\tilde{v} = \sqrt{(b-2\sqrt{\Delta_-})/2}$. There are solitary wave solutions given by:

$$v(\xi) = \pm\frac{\tilde{v}\sqrt{\tanh^2(\xi\bar{v}\sqrt{\bar{v}^2-\tilde{v}^2}/\sqrt{3}) - \bar{v}^2}}{\bar{v}\sqrt{\tanh^2(\xi\bar{v}\sqrt{\bar{v}^2-\tilde{v}^2}/\sqrt{3}) - 1}}$$

CASE 3. $\gamma = 0$

Region $\boldsymbol{b} = \mathbf{1}$, $\boldsymbol{a} < 0$:

There are two orbits homoclinic to origin for system (7) defined by $H(v,y) = 0$ which pass through points $(\pm\sqrt{-2a}, 0)$. Therefore $y = \pm|v|\sqrt{-(v^2 + 2a)/2}$. Two solitary wave solutions are given by:

$$v(\xi) = \pm\sqrt{2a\cot^2(\sqrt{-a}\xi + \pi/2) - 2a}.$$

Region $\boldsymbol{b} = -\mathbf{1}, \boldsymbol{a} > 0$:

There are two heteroclinic orbits of system (7), defined by $H(v,y) = H(\pm\sqrt{a}, 0)$ connecting saddle points $(\pm\sqrt{a}, 0)$ defined by $y = \pm(a - v^2)/\sqrt{2}$. Kink and anti-kink solutions are:

$v(\xi) = \pm\sqrt{a}\tan(\sqrt{a/2}\,\xi)$

CASE 4. Periodic orbits

Now we calculate explicit formulas for bounded periodic travelling waves. Here we only consider periodic orbits of (7) which are located inside the right homoclinic loops of Fig. 2 ($\gamma = -1$) in regions III(a) and III(c) and inside the right heteroclinic loop of Fig. 2 ($\gamma = -1$) in regions III(b). Suppose that the periodic orbit passes through $(\omega_1, 0)$ and $(\omega_2, 0)$ so that $0 < \omega_1 < \omega_2$. Therefore this periodic orbit lie on the level curve $H(v,y) = H(\omega_2, 0) = h$ where H is the Hamiltonian function. Define $G(v,0) = H(\omega_2, 0) - H(v, 0)$. $G(v,0)$ is a sixth order polynomial with respect to v, where $\pm\omega_1, \pm\omega_2, \pm\omega_3$ are their roots with $0 < \omega_1 < \omega_2 < \omega_3$. Therefore,

$$y = \pm\sqrt{2G(v,0)} = \pm\sqrt{(v^2-\omega_1^2)(v^2-\omega_2^2)(v^2-\omega_3^2)/3}.$$

Since $dv/d\xi = y$, we get:

$$\int_0^{\xi} d\zeta = \sqrt{3}\int_{\omega_1}^{v} \frac{d\phi}{\sqrt{(\phi^2-\omega_1^2)(\phi^2-\omega_2^2)(\phi^2-\omega_3^2)}}.$$

With change of variable of the form $\phi^2 = u$ on the right hand side above we can derive

$$\int_0^{\xi} d\zeta = \frac{\sqrt{3}}{2}\int_{\omega_1^2}^{v^2} \frac{du}{\sqrt{u(u-\omega_1^2)(u-\omega_2^2)(u-\omega_3^2)}},$$

Now by using integral tables for elliptic integrals (P. F. Byrd 1971) we have

$$2\xi/\sqrt{3} = g\int_0^{u_1} du = gu_1 = gsn^{-1}(\sin\phi\,, k),$$

where sn^{-1} is inverse Jacobian elliptic function with modulus k (see (P. F. Byrd 1971)), $snu_1 = \sin\varphi$ and

$$\phi = \sin^{-1}\left(\sqrt{\frac{\omega_2^2(v^2-\omega_1^2)}{v^2(\omega_2^2-\omega_2^1)}}\right), k^2 = \frac{(\omega_2^2-\omega_1^2)\omega_3^2}{(\omega_3^2-\omega_1^2)\omega_2^2},$$

$$g = \frac{2}{\sqrt{(\omega_3^2-\omega_1^2)\omega_2^2}}$$

Then after some algebraic calculations we get solitary wave solution:

$$v(\xi) = \frac{\omega_1^2\omega_2^2}{\omega_2^2 + (\omega_1^2-\omega_2^2)sn^2\left(\frac{\xi\sqrt{(\omega_3^2-\omega_1^2)\omega_2^2}}{2}\right)}.$$

Formulas for other periodic orbits of system (7) can be derived in a similar manner and are omitted here for the sake of brevity.

References

Ablowitz, M. J., & Clarkson, P. A. (1991). *Soliton, Nonlinear Evolution Equations and Inverse Scattering.* New York: Cambridge University Press.

Anderson, D. (1983). Variational approach to nonlinear pulse propagation in optical fibers. *Physical review A,* 27(6), 3135–3145.

Byrd, P. F., & Fridman, M. D. (1971). *Handbook of Elliptic Integrals for Engineers and Scientists*. Berlin: Springer-Verlag.

Dai, Z., & Xu., Y. (2011). Bifurcations of travelling wave solutions and exavt solutions to generalized Zakharov equation and Ginzburg-Landau equation. *Applied Mathematics and Mechanics (English Edition)*, 32(12), 1615–1622.

Fan, E. G. (2004). *Integrable Systems and Computer Algebra.* Science Press.

Gambo, B., Boutou, B. T., Kuetche, K. V., & Kofane, T. C. (2010). Dynamical survey of a generalized-Zakharov equation and its exact travelling wave solutions. *Applied Mathematics and Computation*, 217(1), 203–211.

Goldman, M. V. (1984). Strong turbulence of plasma waves. *Reviews of Modern Physics*, 56(4), 709–735.

Hale, J. K., & Kocak, H. (1991). *Dynamics and Bifurcation*. New York: Springer-Verlag.

He, J. H. (2005). Application of homotopy perturbation method to nonlinear wave equations. *Chaos Solitons and Fractals*, 26(3), 695–700.

Hirota, R. (1971). Exact solution of the Korteweg-de Vries equation for multiple collisions of solitons. Physical review letter, 27(18),1192–1194.

Hirota, R. (2004). *The Direct Method in Soliton Theory*. Cambridge: Cambridge University Press.

Hu, J. Q. (2005). An algebraic method exactly solving two high-dimensional nonlinear evolution equations. *Chaos Solitons & Fractals*, 23(2), 391–398.

Kit, E., & Shemer, L. (2002). Spatial versions of the Zakharov and Dysthe evolution equations for deepwater gravity waves. *Journal of Fluid Mechanics*, 450(1), 201–205.

Kuznetsov, Y. A. (1998). *Elements of Applied Bifurcation Theory*. NewYork: Springer-Verlag.

Liu, S. K., Fu, Z. T., Liu, S. D., & Zhao, Q. (2001). Jacobi elliptic function expansion method and periodic wave solutions of nonlinear wave equations. *Physics Letters A*, 285(5-6), 69–74.

Olver, P. J. (1993). *Applications of Lie Groups to Differential Equations*. NewYork: Springer.

Rogers, C., & Schief, W. K. (2002). *Bäcklund and Darboux Transformations, Geometry and Modern Applications in Soliton Theory*. Cambridge: Cambridge University Pre.

Wang, M. L. (1996). Exact solutions for a compound KdV-Burgers equation. *Physics Letters A*, 224(1), 279–287.

Yan, C. T. (1996). A simple transformation for nonlinear waves. *Physics Letters A*, 224(1), 77–84.

Zakharov, V. E., & Shabat, A. B. (1972). Exact theory of two-dimensional self-focusing and one dimensionsl self-modulation of waves in nonlinear media. *Journal of Experimental and Theoretical Physics*, 34(1), 62–69.

Zakharov, V. E. (1972). Collapse of Langmuir waves. Soviet Physics-JETP. 35(5), 908–914.

Zakharov, V. E., Synakh, V. S. (1976). The nature of the self-focusing singularity. Soviet Physics-JETP, 41(3), 465–468.